CFD ANALYSIS OF ENHANCEMENT OF TURBULENT FLOW HEAT TRANSFER IN A HORIZONTAL CIRCULAR TUBE WITH DIFFERENT INSERTS

Sajid Hussein Ali Al – Abbasi
Lecturer, Department of Mechanical Engineering College of Engineering, University of Basrah, Iraq

Abstract

The present work includes the results of CFD analysis of enhancement of turbulent flow heat transfer in a horizontal circular tube with different shapes of inserts (disc, diamond and trapezoidal), with air as working fluid. The Reynolds number ranged from 6000 to 14000.

It is observed that enhancement of heat transfer as compared to the conventional bare tube at the same mass flow rate was found to be a factor of 3 to 5 times, were as the friction factor rise was about a factor of 5 times for different tube inserts.

Finally we compared results with theoretical values (DITTUS-BOELTER EQUATION**)** by using tool of package of ANSYS-FLUENT. Geometries for plain tube, and tube with different inserts is developed in ICEM CFD (3D) with fine meshing and exported to ANSYS-FLUENT, then suitable boundary conditions are applied to these models and solved energy, momentum and turbulence equations and results obtained are discussed.

Keywords: Inserts, Reynolds number, Nusselt number (Heat transfer coefficient), Friction factor, Turbulent flow, and Enhancement Efficiency (Friction factor ratio).

1. Introduction

Heat transfer enhancement or intensification is the study of improved heat transfer performance. Recently adequate energy source and material costs have provided significant resources for the development of enhanced energy efficient heat exchangers. As a result, considerable emphasis has been placed on the development of various augmented heat transfer surfaces and devices. An enhanced surface is more efficient in transferring heat than what might be called as a standard surface. While considering the associated flow

friction change is also to be taken into account. Analogies between momentum and heat transfer show that increasing the friction factor increases the heat transfer coefficient.

The moody chart shows that in turbulent flow increasing the relative roughness of the surface increases the friction factor. This chart is based on the random sand grain type of source roughness. Surface roughness can be produced by the machining of the surface as well as casing, forming, and welding processes. Other types of surface have been produced, and their friction factors and heat transfer characteristics have been tested for possible use in heat transfer augmentation.

The use of fins on the outer surface of tube enhance heat transfer is well known. Internally finned tubes have been used also to enhance heat transfer to fluids flowing inside tubes. Heat transfer and friction factor correlations have been presented for internally finned tubes under laminar and turbulent flow conditions.

Enhancement devices such as twisted taps have been employed in the form of inserts into the tubes to promote increased heat transfer for the laminar and turbulent flow of viscous fluid.

Coiled tubes can serve as a heat transfer enhancement device because the secondary flow produced by the curvature causes an increase in the heat transfer coefficient. In general, enhancing the heat transfer can be divided into two groups.

Passive method, without stimulation by the external power such as a surface coating, rough surfaces, extended surfaces, swirl flow devices, the convoluted (twisted) tube, additives for liquid and gases.

The other is the active method, which requires extra external power sources, for example, mechanical aids, surface-fluid vibration, injection and suction of the fluid, jet impingement, and use of electrostatic fields.

Passive heat transfer enhancement techniques (for example, wall roughness, swirl flow inducement, and inserts) are preferred over active (for example, surface vibration, electro-static fields) ones to obtain more compact heat exchangers and to reduce energy costs.

The increasing heat transfer with augmentation is accompanied by an increase in the friction factor. In some situations the heat transfer coefficients are increased at most about 4 times while the friction factors are increased as much as 50% or more. An increased friction factor implies an increased power for pumping the fluid. For a given enhancement technique, if the heat transfer and the friction factor data are available as a function of the Reynolds number, it may be possible to optimize the system to reduce the heat transfer surface, to obtain increased heat transfer capacity and to reduce the power required for pumping the fluid.

The great attempt on utilizing different methods is to increase the heat transfer rate through the compulsory forced convection. Meanwhile, it is found that this way can reduce the sizes of the heat exchanger device and save up the energy. Heat transfer enhancement today is characterized by rigorous research activities both in academic and industrial levels. (Prasad and Shen, 1993) proposed a new criterion for evaluating the effectiveness of a passive heat transfer enhancement device. (Prasad and Shen, 1994) studied the enhancement of heat transfer by using several coil-wire inserts based on exergy analysis. Twelve different coil-wire inserts were tested in turbulent flow regions. (Ravigururajan and Bergles, 1996) presented the general correlations for the friction factor and heat-transfer coefficient for the single-phase turbulent flow in internally augmented tubes. Different types of commercial ribbed tubes were tested under heating conditions. (Agrawal et al. 1998) experimentally studied the heat transfer enhancement by coiled wire inserts during the forced convection condensation of R-22 inside horizontal tubes. Three different wire diameters and three different coil pitches were used in full length of the test-condenser. (Kim et al. 2001) visualized the flow pattern, void fraction and slug rise velocity on the counter-current two-phase flow in a vertical round tube with coil-wire inserts. (Wang and Sund, 2002) studied the heat transfer enhancement technology in the heat exchanger. (Rahai and Wong, 2002) experimentally studied the turbulent jets from round tubes with coil inserts. Recently, (V. Ozceyhan, 2005) numerically studied the conjugate heat transfer and thermal stress in the tube with coil-wire inserted tube under uniform wall heat flux. A finite difference scheme was employed to solve the energy and governing flow equations.

Compared to a smooth tube, internal spiral grooves impart swirl to the essentially axial flow in the vicinity of the tube wall as well as provide benefits of surface roughness (groove height is typically smaller than the laminar sub-layer thickness in a turbulent flow) (Webb et al. 2000) . Probably (Choi, 1995) at the Argonne National Laboratory was the first to employ particles of nanometer dimension suspended in solution as nanofluid and showed considerable increase in the nanofluid thermal conductivity. (Yun et al. 2007) also reported the same observations in their study of flow boiling heat transfer characteristics of nitrogen in coiled wire inserted tubes. The Experimental investigations of Hsieh and Liu report that Nusselt numbers were between four and two times of the bare tube at low Re number value.

The present study attempts to theoretically investigate the heat transfer characteristics and friction factor of air flowing through a horizontally circular tube with different inserts like a disc (cylinder), trapezoidal, and diamond inserts. Previous studies have not been addressed

heat transfer in tubes with disc, trapezoidal and diamond inserts through the range of turbulent flow regime.

Sequence of Operation:

Without Inserts:

Initially the CFD experiment is carried out with air as the moving fluid through pipe section without any inserts.

With Insert:

Three geometries of inserts are considered for CFD analysis i.e. Disc insert, Trapezoidal insert and Diamond insert.

2. Computational Fluid Dynamics Modeling

CFD provides numerical approximation to the equations that govern fluid motion. Application of the CFD to analyze a fluid problem requires the following steps. First, the mathematical equations describing the fluid flow are written. These are usually a set of partial differential equations. These equations are then discretized to produce a numerical analogue of the equations. The domain is then divided into small grids or elements. Finally, the initial conditions and the boundary conditions of the specific problem are used to solve these equations. The solution method can be direct or iterative. In addition, certain control parameters are used to control the convergence, stability, and accuracy of the method. All CFD codes contain three main elements: (1) A pre-processor, which is used to input the problem geometry, generate the grid, and define the flow parameter and the boundary conditions to the code. (2) A flow solver, which is used to solve the governing equations of the flow subject to the conditions provided. (3) A post-processor, which is used to massage the data and show the results in graphical and easy to read format.

The equations governing the fluid motion are the three fundamental principles of mass, momentum, and energy conservation.

Continuity $$\frac{\partial \rho}{\partial t} + \nabla.(\rho V) = 0 \qquad (2.1)$$

Momentum $$\rho \frac{DV}{Dt} = \nabla.\tau_{ij} - \nabla p + \rho F \qquad (2.2)$$

Energy $$\rho \frac{DE}{Dt} + p(\nabla.V) = \frac{\partial Q}{\partial t} - \nabla.q + \Phi \qquad (2.3)$$

where **ρ** is the fluid (air) density, ***V*** is the fluid (air) velocity vector, τ_{ij} is the viscous stress tensor, ***p*** is pressure, **F** is the body forces, **E** is the internal energy, ***Q*** is the heat source term, ***t*** is time, **Φ** is the dissipation term**,** and **∇. q** is the heat loss by conduction.

2. 1 Geometry Description and Meshing

Geometry of the tube with inserts is modeled in ICEM CFD (Integrated computer aided Engineering and Manufacturing) software. This tool is an advanced preprocessor tool which is used to meet the specific geometry and meshing needs. ICEM CFD is used in order to mesh the components. In this tool the meshing is basically classified in two categories.

i. Hexa meshing
ii. Tetra Meshing

Hexa meshing is composed of filling the volume of the geometry with cuboids. The ends of these cuboids can have arbitrary curvatures. These cuboids are called as Hexa elements. These hexa elements are closed with six faces which are called as quad elements. Details of tetra meshing are not discussed as they are not used in the present project.

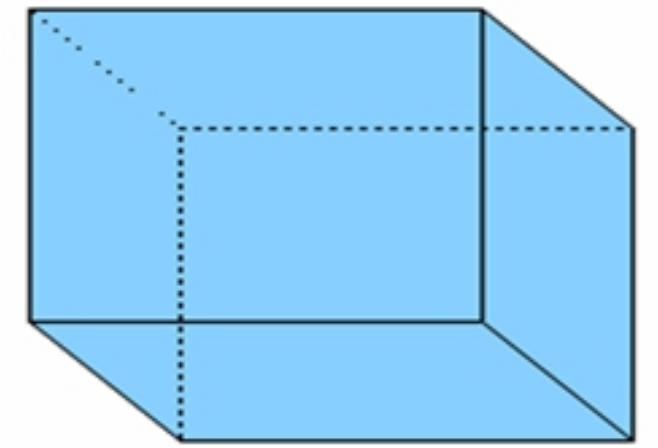

Hexa Element.

Meshing of the geometry is done using blocking concept. ICEM CFD Hexa allows us to generate high quality hexahedral elements with less time. Blocking is parametric and can be fit to topologically similar geometries. This means we shouldn't have to block the same model type twice because you can fit your previous blocking to the new geometry. These blocks will be subdivided with nodes such that the volume is filled with hexa elements.

2. 2 Ansys-Fluent Setup

The first steps taken after importing the mesh geometry into ANSYS-FLUENT involve checking the mesh/grid for errors. Checking the grid assures that all zones are present and all dimensions are correct. It is also important to check the volume and make sure that it is not negative. If the volume is shown as negative, there is a problem with the grid. When the grid is checked completely and free of errors, a scale and units can be assigned. For this study, the grid was created in mm, and then scaled to

meters. Once the grid was set, the solver and boundary conditions of the system were then set and cases were run and analyzed.

2. 3 Defining The Models

To run the cases, the model properties must be set. Model properties include the internal ANSYS-FLUENT solver settings like air and thermal properties, as well as model operating conditions and grid boundary conditions. The following settings were used to create the model in ANSYS-FLUENT.

1. 3D
2. Steady state
3. Enabling energy

2. 4 Defining the Material Properties

This section of the input contains the options for the materials to be chosen for the air is passing in the tube with heating coil. Properties that can be specified in this section are density, viscosity, specific heat, and thermal conductivity. Air is passed through the tube and due to the heat transfer from heating coil the air gets heated up. Figure1 shows the construction of tube.

Figure1: 3D Overview of Plain Tube.

For natural convection cases, density is the driving mechanism for air motion. In ANSYS-FLUENT different density models can be incorporated. Since for the present project the temperature variations should be there from start point to end point, thus the properties viscosity, specific heat and thermal conductivity are considered varying with temperature. Polynomial curve fit equations are incorporated in ANSYS-FLUENT for varying properties.

2. 5 Defining the Operating Conditions

The operating conditions include gravity and pressure. Gravity can be entered in values of m/s^2 in x and y and z components. In this project, the geometry was modeled assuming air will be placed on the ground with gravity acting downwards in the Y direction.

2. 6 Defining the Boundary Conditions

Proper specification of the boundary conditions is a vital step in accurately modeling air flow system. In ANSYS-FLUENT, boundary conditions must be specified at each surface defined in the mesh generation

process. Specifically, information about the mass flow rate, velocity and temperature must be specified at each surface. For surfaces that have been defined as "walls," for tube is considered as adiabatic walls with same heat flux. For surfaces that have been defined as "mass flow inlets" are specified with corresponding flow rates in to the tube. For the surfaces defined with "velocity inlets" are specified as negative velocities coming out of tube. Negative velocities are computed based on the continuity equation. For the modeling performed in this study, the boundary conditions are summarized in Table 1 **Error! Reference source not found.** Once all the models, operating conditions and boundary conditions are specified, the ANSYS-FLUENT code can be executed.

Table 1: Boundary condition specification for ANSYS-FLUENT

Zone	**Type**	**Boundary Conditions**
Tube	Wall	Heat flux = 759.010 w/m^2
Inlet temperature	Heat inlet	Temperature = 53.3^0c
Mass Flow rate	Inlet	0.00334, 0.004108, 0.00474 and 0.005304kg/sec
Pressure	Outlet	101395.8 Pa

2. 7 Executing the Ansys-Fluent Code

Each case must be initialized before the ANSYS-FLUENT code begins iterating toward a converged solution. Initializing the case essentially provides an initial guess for the first iteration of the solution. In the initialization process, the user must specify which zones will be provided with initial conditions. For the modeling performed in this study the option chosen was to compute from inlet. The final initialization step is for the user to enter the maximum number of iterations, after which the simulation begins. For the modeling performed in this study, the number of iterations ranged between 500 and 1000 depending on the case being run and how long it took to converge the solution.

3. Description of the Problem and Geometry

The primary goal of the present work is to enhance the heat transfer in a tube employing various inserts. Also determine average Nusselt number and friction factors for Reynolds number ranging from 6000-14000 in the turbulent region. Average Nusselt numbers, friction factors of working fluid (air) flowing in the plain tube are compared with average Nusselt numbers, friction factors of working fluid (air) flowing in tube with disc (cylinder), trapezoidal and diamond inserts which enhance heat transfer. Enhancement Efficiencies of the different inserts also compared. The geometry of the tube and dimensions of the insert used in this study are listed:

Inner Diameter of the test pipe, $D = 2.75*10^{2}$ m

Cross-sectional area of the pipe, $A_p = 5.939572*10^{-4}$ m^2

Length of the Heating Zone, $L = 61*10^{-2}$ m

Diameter of the Orifice, $d_0 = 14*10^{-3}$ m
Cross-sectional area of the Orifice, $A_o = 1.54*10^{-4}$ m^2
Coefficient of discharge, $C_d = 64*10^{-2}$
Thickness of the insert, th = $2*10^{-3}$ m
Pitch = 50 mm
Core rod diameter = $2*10^{-3}$ m

CFD techniques used to perform the overall performance and optimization analysis of the fluid flow transfer of the tube with/without insert was performed using ANSYS-FLUENT.

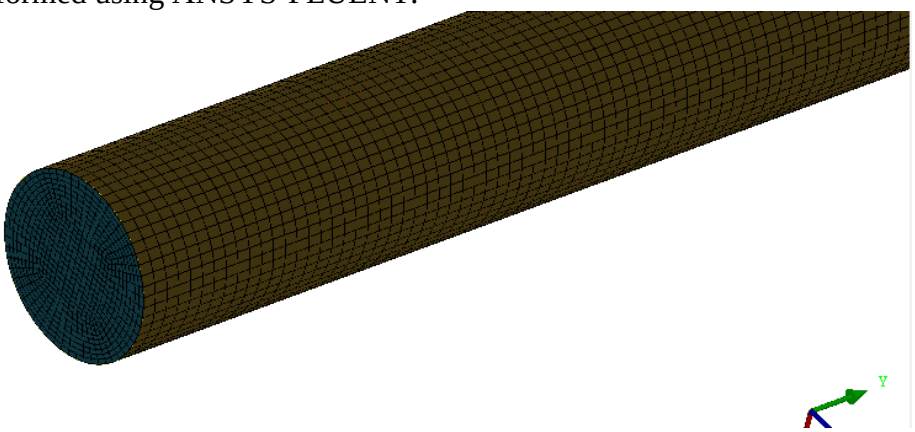

Figure 2: Grid for the Plain Tube configuration
Grid Info:
Cells: 232092

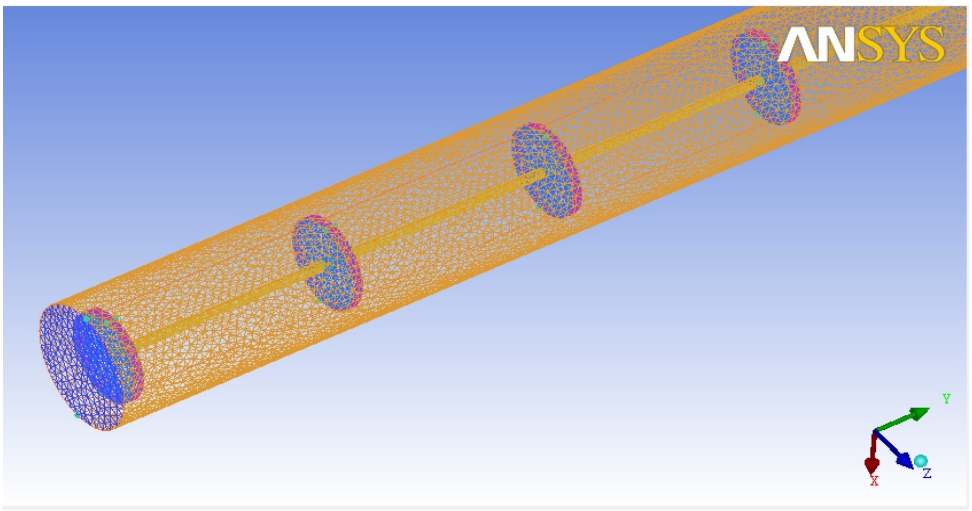

Figure 3 : Grid for the Tube with disc (cylinder) insert configuration
Grid Info:
Cells: 852465
Disc (cylinder) diameter = 20 mm

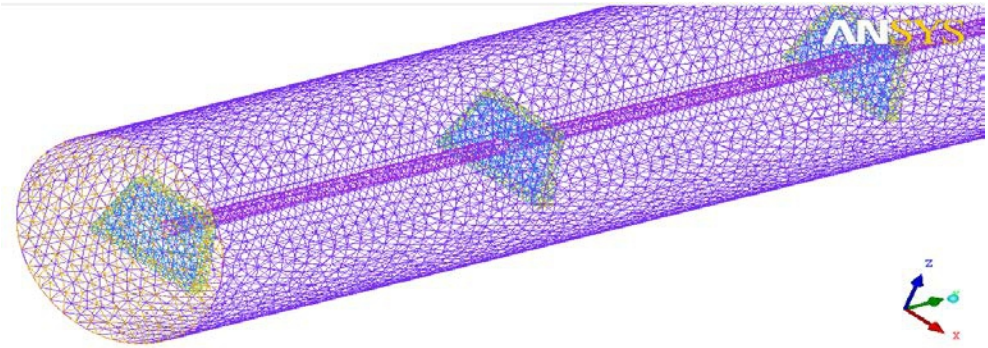

Figure 4: Grid for the Tube with trapezoidal insert configuration
Grid Info:
Cells: 833004
Trapezoidal bottom length = 15 mm
Trapezoidal top length = 10 mm
Trapezoidal height = 10 mm

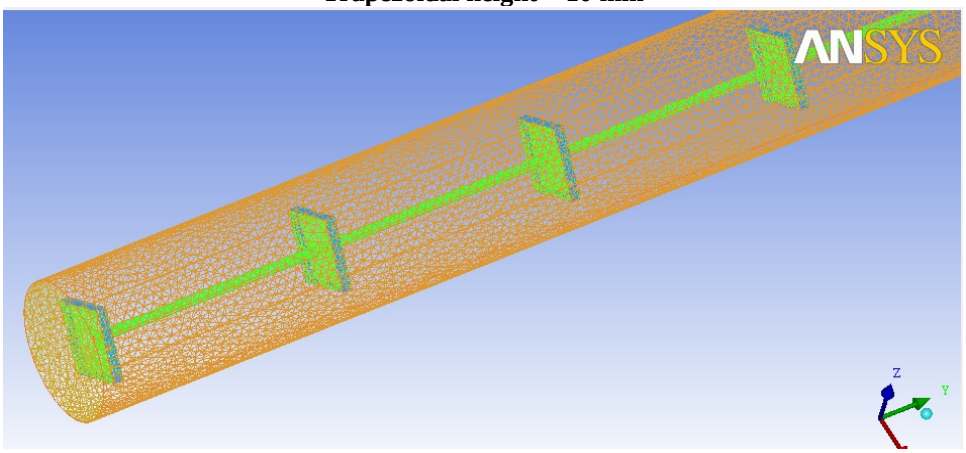

Figure 5: Grid for the Tube with diamond insert configuration
Grid Info:
Cells: 833722
Diamond diagonal length = 20 mm
Grid Independence check:

We have also refined mesh to a finer mesh and observed that results obtained didn't have much difference, so we have considered above grid size to be optimal one for present analysis.

4. ANALYSIS OF PROBLEM IN ANSYS-FLUENT

Sequence of steps involved in ANSYS-FLUENT and analysis:

1. Determination of Mean Velocity (V) of working fluid (air) by using Reynolds Number considered from the following Eq.

$Re=\rho V D_i/\mu$

2. Nusselt number and friction factor are calculated by equations are given below:

$Nu=hD_i/k$

$h=((Q/A)/(T_w-T_b))$

Where T_w= Average Surface Temperature

$T_b=(T_i+T_0)/2$

$f=((\Delta P)/(L/D)\ \rho V^2/2)$

3. Enhancement Efficiency is calculated using the following equation:

Friction factor ratio = $(Nu/Nu_0)/(f/f_o)^{1/3}$

5. Theoretical Calculations:

Nusselt number and friction factor are calculated for Reynolds numbers ranging from 6000-14000 by using **DITTUS-BOELTER** results are tabulated below:

Nusselt number:

$Nu=0.023 \times Re^{0.8} \times Pr^{0.4}$ for $6000 \leq Re \leq 14000$

Friction factor:

f= $[1.82 \log_{10} Re-1.64]^{-2}$ for $6000 \leq Re \leq 14000$

Table 2: Theoretical Calculations

S. No	Mass flow rate	Re	F	Nu
1	0.003334	7757.98	0.0338	25.79
2	0.004108	9557.67	0.0316	30.48
3	0.00474	11028.08	0.0303	34.17
4	0.005304	12341.18	0.0295	37.39

ANSYS-FLUENT Calculations:

In ANSYS-FLUENT also cases are analyzed separately one for plain tube, other for tube with disc (cylinder), trapezoidal and diamond inserts respectively. The calculations for these cases are tabulated below.

Table 3: Plain Tube Calculations in ANSYS-FLUENT

S. NO	Mass flow rate	Tw (Avg. Wall temperature) K	Tb (K)	Q/A	Re	Nu	Pressure drop **ΔP** (Pa)	h (w/m^2-K)	f
1	0.003334	363.983	335.406	759.01	7757.98	23.8017	11.4221	24.7266	0.038733
2	0.004108	357.656	334.118	759.01	9557.67	28.4486	16.876	29.5541	0.037694
3	0.00474	354.168	332.848	759.01	11028.08	31.4305	21.7285	32.6519	0.036453
4	0.005304	351.706	332.193	759.01	12341.18	34.2683	26.5954	35.6000	0.035634

Table 4 : Plain Tube with Trapezoidal inserts Calculations in ANSYS-FLUENT

S. NO	Mass flow rate	Tw (Avg. Wall temperature) K	Tb (K)	Q/A	Re	Nu	Pressure drop ΔP (Pa)	h (w/m^2-K)	f
1	0.003334	355.796	331.630	759.01	7757.98	30.6313	84.207	31.8216	0.2855
2	0.004108	351.179	328.120	759.01	9557.67	35.9875	123.731	37.3859	0.2763
3	0.00474	348.821	326.920	759.01	11028.08	40.2445	161.399	41.8083	0.2707
4	0.005304	346.460	326.194	759.01	12341.18	43.9761	199.066	45.6849	0.2667

Table 5: Plain Tube with Diamond inserts Calculations in ANSYS-FLUENT

S. NO	Mass flow rate	Tw (Avg. Wall temperature) K	Tb (K)	Q/A	Re	Nu	Pressure drop ΔP (Pa)	h (w/m^2-K)	f
1	0.003334	348.356	340.591	759.01	7757.98	44.7463	210.720	46.4851	0.7145
2	0.004108	344.797	336.692	759.01	9557.67	52.7770	311.489	54.8279	0.6957
3	0.00474	342.685	334.513	759.01	11028.08	59.1738	407.711	61.4732	0.6840
4	0.005304	341.191	333.100	759.01	12341.18	64.7826	504.144	67.3000	0.6754

Table 6 : Plain Tube with Disc (cylinder) inserts Calculations in ANSYS-FLUENT

S. NO	Mass flow rate	Tw (Avg. Wall temperature) K	Tb (K)	Q/A	Re	Nu	Pressure drop ΔP (Pa)	h (w/m^2-K)	f
1	0.003334	342.745	343.580	759.01	7757.98	68.8613	641.083	71.5372	2.1739
2	0.004108	339.982	339.640	759.01	9557.67	81.7430	953.987	84.9194	2.1308
3	0.00474	338.357	337.360	759.01	11028.08	91.9827	1253.98	95.5570	2.1037
4	0.005304	337.215	335.842	759.01	12341.18	101.046	1552.22	104.973	2.0797

Table 7: Nusselt number calculations for different inserts

Mass flow rate	Re	Trapezoidal (Nu/Nu_0)	Diamond (Nu/Nu_0)	Disc (cylinder) (Nu/Nu_0)
0.003334	7757.98	1.286936106	1.879960804	2.893119698
0.004108	9559.023	1.264998522	1.855166685	2.873349743
0.00474	11029.64	1.280426341	1.882684053	2.926539091
0.005304	12342.03	1.283285181	1.890450434	2.948689579

Table 8: Friction factor calculations for different inserts

Mass flow rate	Re	Trapezoidal $(f/f_0)^{1/3}$	Diamond $(f/f_0)^{1/3}$	Disc(cylinder) $(f/f_0)^{1/3}$
0.003334	7757.98	1.946265665	2.642327227	3.828741986
0.004108	9559.023	1.942687752	2.642760047	3.837876364
0.00474	11029.64	1.95114868	2.657301876	3.864443433
0.005304	12342.03	1.95612613	2.666343054	3.878962515

Table 9: Overall enhancement ratio for different inserts

Mass flow rate	Re	Trapezoidal	Diamond	Disc (cylinder)
0.003334	7757.98	0.661269	0.711501	0.755639
0.004108	9559.023	0.65121	0.701995	0.748686
0.00474	11029.64	0.656302	0.708496	0.757306
0.005304	12342.03	0.656052	0.709034	0.760177

CFD RESULTS AND ANALYSIS

Each case was run using higher order residual schemes for each governing equations. It was ensured that residuals dropped to at least 10^{-6} for each case. Nusselt number and friction factor for plain tube are validated with theoretical relations and then they are determined for disc (cylinder), trapezoidal, and diamond insert. Nusselt number and friction factor calculated for the plain tube and plain tube with different insert for 6000<Re<14000. The Nusselt number and friction factor obtained for the tube with insert are compared with Nusselt number and friction factor of Plain tube.

Each case is solved for 3 equations Energy, Momentum and Turbulence and results are plotted on corresponding graphs as shown below.

Figures 6: Static Temperature Variations for the Plain Tube configuration on wall

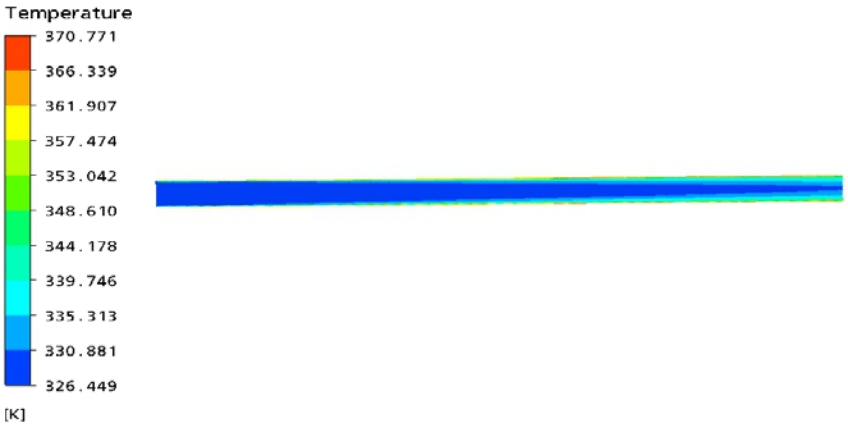

Figures 7: Static Temperature Variations for the Plain Tube configuration on center plane (Maximum temperature is found to be is 370.71 K)

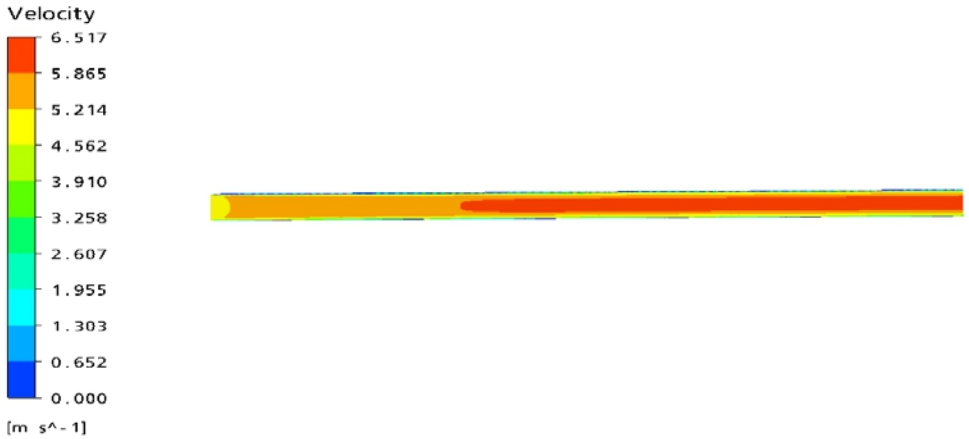

Figure 8: Velocity Variation for the Plain Tube configuration

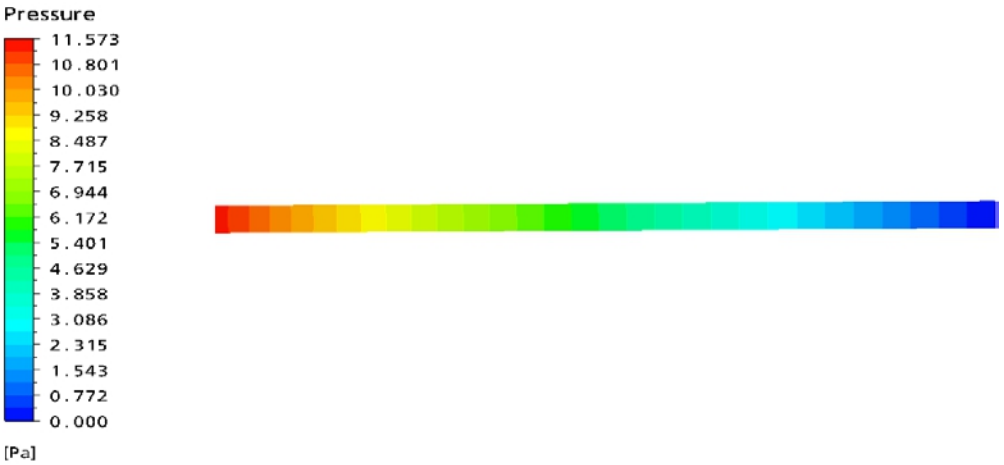

Figure 9: Pressure Variation for the Plain Tube configuration

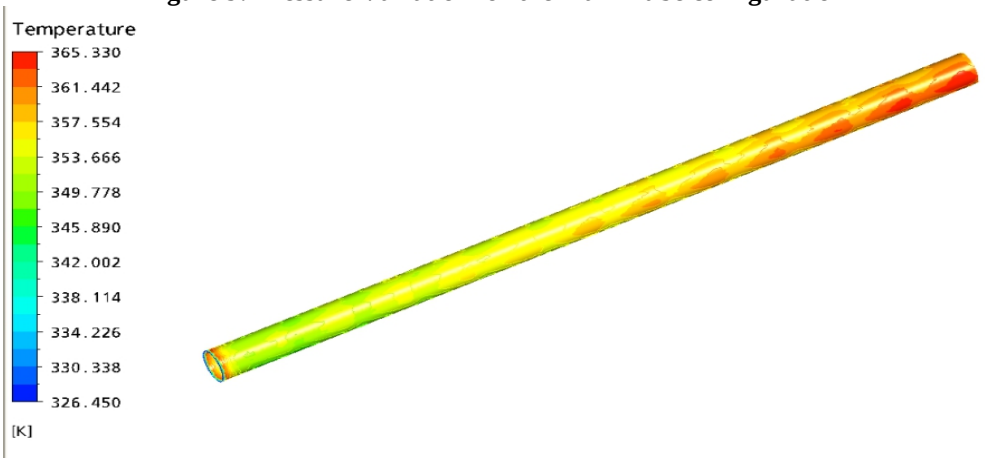

Figure 10: Temperature Variation for the Tube with trapezoidal insert configuration on wall

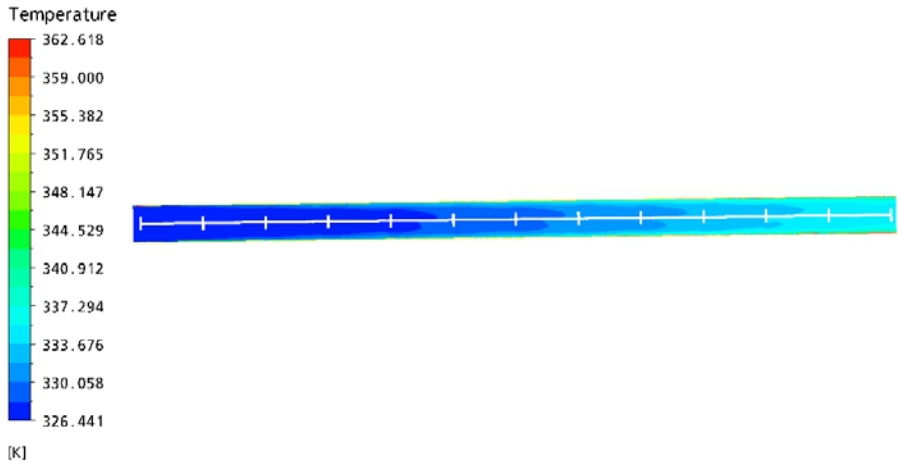

Figure 11: Temperature Variation for the Tube with trapezoidal insert configuration on center plane

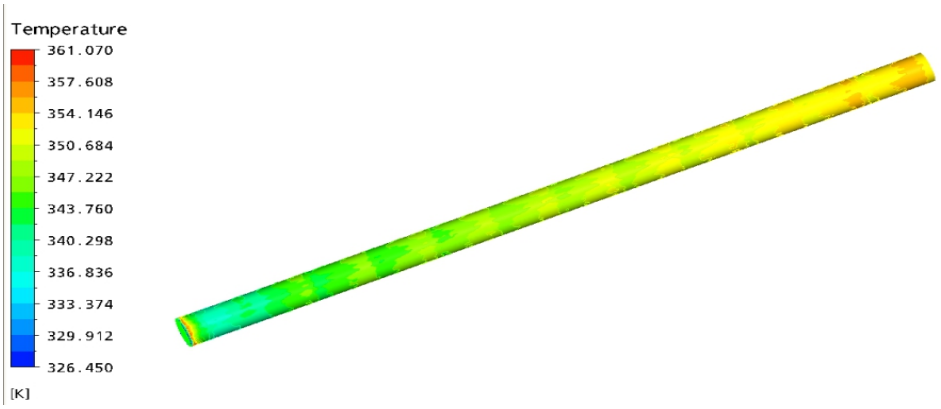

Figure 12: Temperature Variation for the Tube with diamond insert configuration on wall

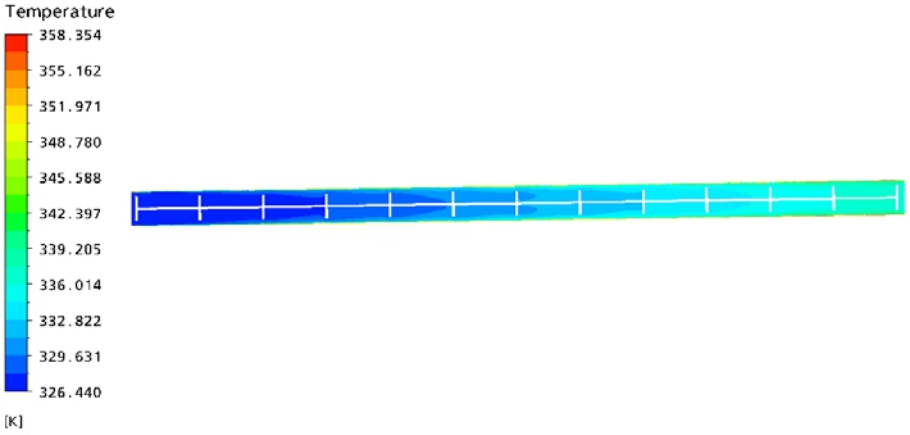

Figure 13: Temperature Variation for the Tube with diamond insert configuration on center plane

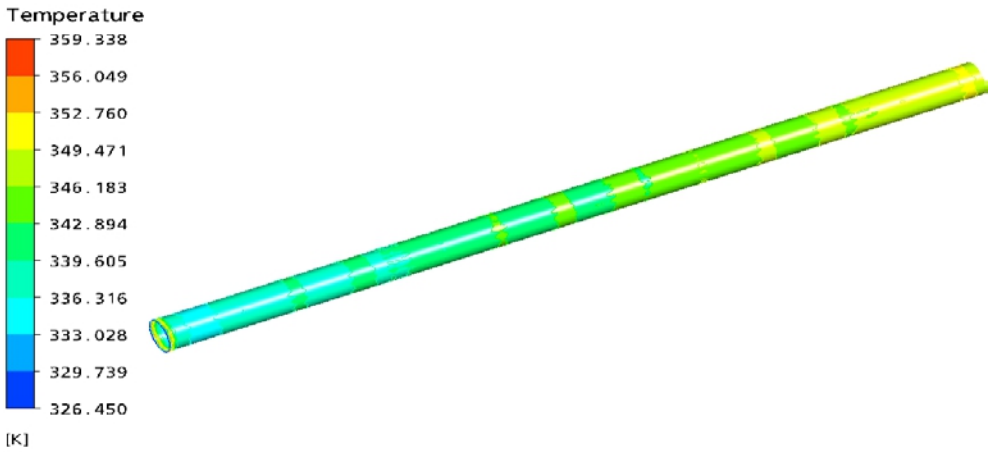

Figure 14: Temperature Variation for the Tube with disc (cylinder) insert configuration on wall

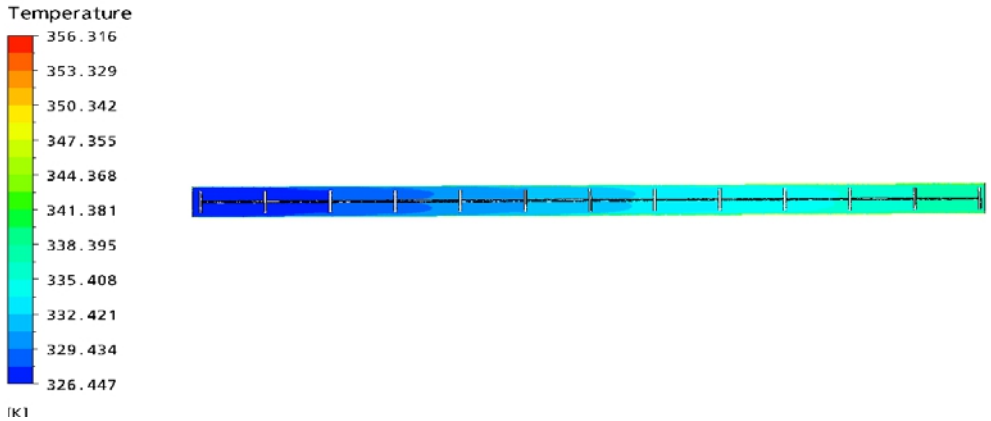

Figure 15: Temperature Variation for the Tube with disc (cylinder) insert configuration on center plane

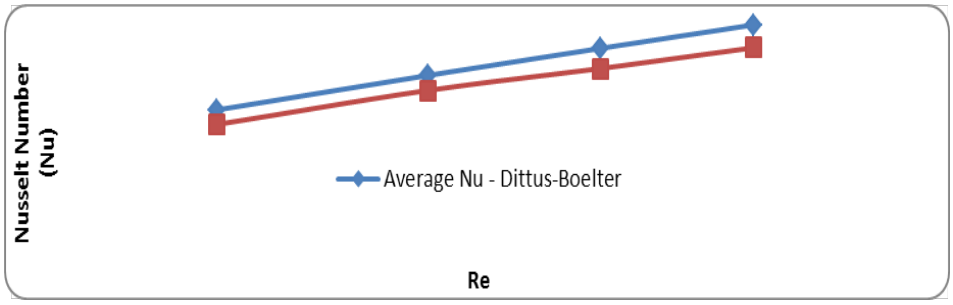

Graph 1: Variationof Nusselt number Vs Re

Comparison graph between Theoretical and CFD Analysis for Variation of Average Nusselt Number with Reynolds number in Plain Tube.

Inference from Graph

Above graph reveals that results obtained through ANSYS-FLUENT are almost identical with values thorugh DITTUS-BOELTER for Nusselt number. The Maximum % variation of CFD results for Nusslet number is found to be 6.1% with respect to theoretical values.

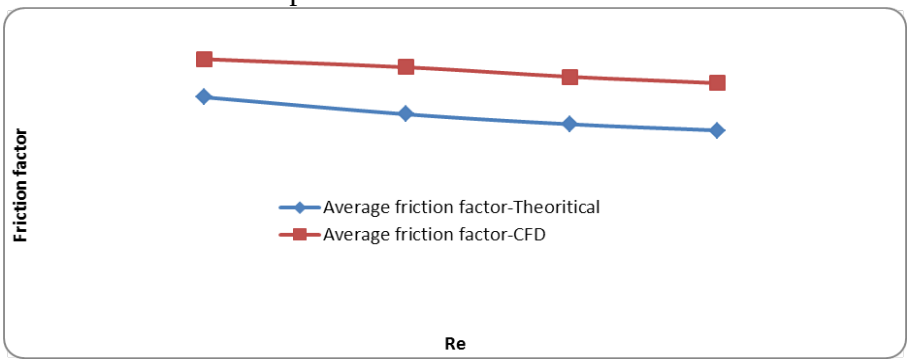

Graph 2: Variationof Friction factor Vs Re

Comparison graph between Theoretical and CFD Analysis for Variation of Friction Factor with Reynolds number in Plain Tube.

Inference from Graph

Above graph reveals that results obtained through ANSYS-FLUENT are well within the range of values obtained through DITTUS-BOELTER for Friction Factor. The Maximum % variation of CFD results for Friction Factor is found to be 10.3% with respect to theoretical values.

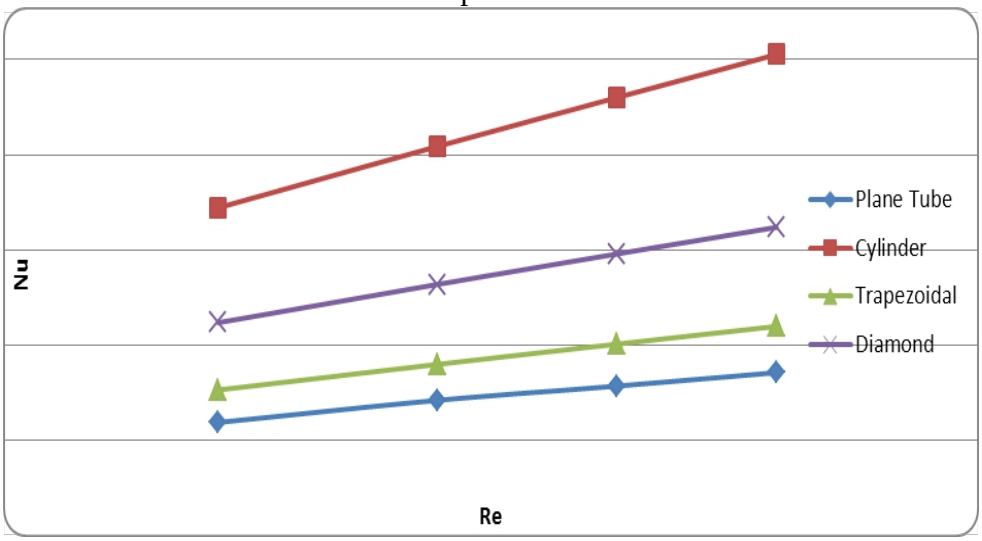

Graph 3: Variationof Nusselt number Vs Re with different inserts

Comparison graph between CFD Analysis for Variation of Nusselt Number with Reynolds number in Plain Tube Vs different insert

Inference from Graph:

Above graph reveals that results obtained through ANSYS-FLUENT. The maximum % variation of CFD results for Nusselt Number is found to 87% for disc (cylinder) insert, 85% for diamond insert and 28% of trapezoidal insert, with respect to Plain Tube.

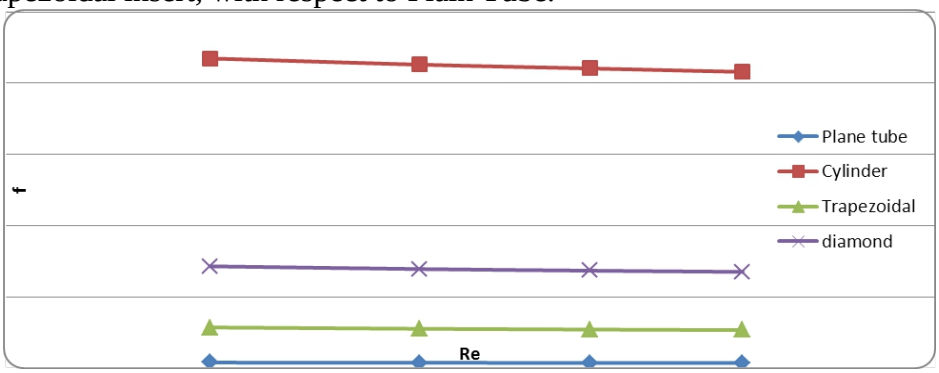

Graph 4: Variationof frictionfactor Vs Re with different inserts

Comparison graph between CFD Analysis for Variation of Friction factor with Reynolds number in Plain Tube Vs different inserts.

Inference from Graph:

Above graph reveals that results obtained through ANSYS-FLUENT. The max 600 % variation of CFD results for Friction factor is found for disc (cylinder) insert with respect to Plain Tube.

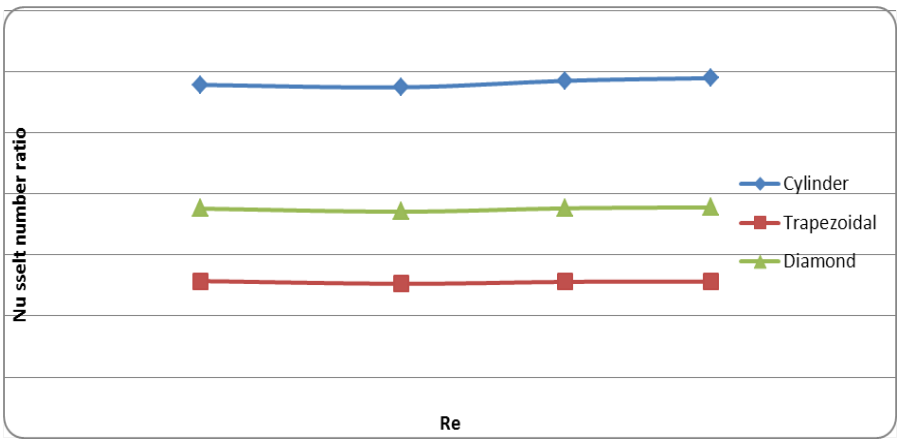

Graph 5: Variationof Nusselt number ratio Vs Re with different inserts

Comparison graph between the Nusselt Number ratio Vs Reynolds Number of CFD values of different inserts through Ansys-FLUENT.

Inference from Graph:

Above graph reveals that if Reynolds number increases Nusselt number ratio also increasing. Maximum Enhancement of Nusselt Number for disc (cylinder) insert is 2.8.

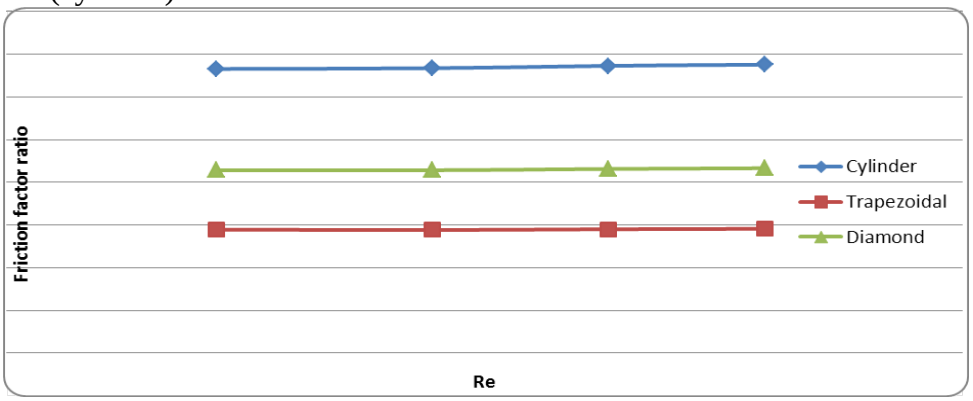

Graph 6: Variationof friction factor Vs Re with different inserts

Comparison graph between the Friction Factor ratio Vs Reynolds Number of CFD values of different inserts through ANSYS-FLUENT.

Inference from Graph

Above graph reveals that if Reynolds number increases friction factor is decreasing. Minimum friction factor ratio for trapezoidal insert is 1.95.

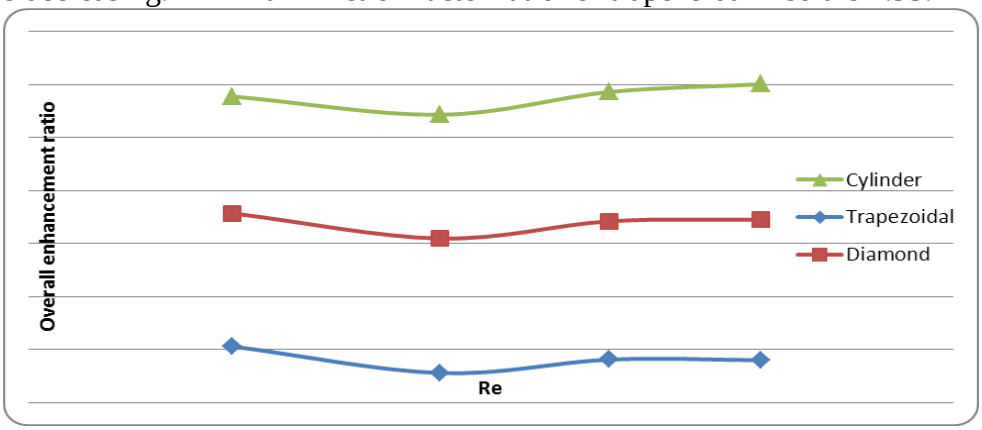

Graph 7: Variation of Overall enhancement ratio Vs Re with different inserts

Comparison graph between the Overall enhancement ratio Vs Reynolds Number of CFD values of different inserts through ANSYS-FLUENT.

Inference from Graph:

Above graph reveals that overall enhancement ratio is high (0.75) for disc (cylinder) and low (0.65) for Trapezoidal insert

Conclusion

In the present work CFD Analysis of enahancement of heat transfer of different inserts for improving heat transfer in horizontal tube has been carried out with boundary conditions such as mass flow rate inlet and pressure outlet defined with constant heat flux. Mesh is created ICEM CFD (3- dimensional). The variations of Temperatures, average Nusselt Numbers, friction factor and presurre drop on with inserts like diamond, trapezoidal and disc (cylinder) has been studied. Results revelaed that average Nusselt Numbers and friction factors are considerably more with different inserts when compared to plain tube.

Improvement of average Nusselt Numbers for tube with 87% for disc (cylinder) insert, 85% for diamond insert and 28% for trapezoidal insert, with respect to Plain Tube. Similarly friction factor for tube with disc (cylinder) insert is 600% more compared with the plain tube. Overall enhancement ratio is high (0.75)for disc (cylinder) insert and low(0.65) for Trapezoidal insert.

Future work

CFD simulation can work with different inserts as well as different Reynolds number. Also can carry out the experimental studies to validate the present results.

NomenclatureGreek conventions

A Surface area in m^2 μ Dynamic viscosity of fluid kg/m.s.

D_i Inner diameter of tube in m ρ Density in Kg/m^3.

Do Outer diameter of tube in m.

f Friction Factor for Tube with insert.

f_0 Friction Factor for Plain tube.

h Heat transfer coefficient in $W/m^2.C°$.

k Thermal Conductivity in W/m. $C°$.

L Length of tube in m.

N_u Average Nusselt Number for Tube with insert.

N_{uo} Average Nusselt Number for Plain Tube.

Δp Pressure Drop.

Q Heat supplied in W.

Re Reynolds number

T_i Inlet temperature in $C°$.

T_0 Outlet temperature in $C°$.

Tb Bulk temperature in $C°$.

T_w Inner surface temperature in $C°$.
V Mean velocity of fluid in m/s.

References:

R.C. Prasad, J. Shen, Performance evaluation of convective heat transfer enhancement devices using exergy analysis, International Journal of Heat and Mass Transfer 36 (1993) 4193–4197.
R.C. Prasad, J. Shen, Performance evaluation using exergy analysis–application to wire-coil inserts in forced convection heat transfer, International Journal of Heat and Mass Transfer 37 (1994) 2297–22303.
T.S. Ravigururajan, A.E. Bergles, Development and verification of general correlations for pressure drop and heat transfer in single-phase turbulent flow in enhanced tubes, Experimental Thermal and Fluid Science 13 (1996) 55–70. 762 P. Naphon / International Communications in Heat and Mass Transfer 33 (2006) 753–763.
K.N. Agrawal, A. Kumar, M.A.A. Behabadi, H.K. Varma, Heat transfer augmentation by coiled wire inserts during forced convection condensation of R-22 inside horizontal tubes, International Journal of Multiphase Flow 24 (1998) 635–650.
H.Y. Kim, S. Koyama, W. Matsumoto, Flow pattern and flow characteristics for counter-current two-phase flow in a vertical round tube with wire-coil inserts, International Journal of Multiphase Flow 27 (2001) 2063–2081.
L. Wang, B. Sund, Performance comparison of some tube inserts, International Communication Heat Mass Transfer 29 (2002) 45–56.
H.R. Rahai, T.W.Wong, Velocity field characteristics of turbulent jets from round tubes with coil inserts, Applied Thermal Engineering 22 (2002) 1037–1045.
V. Ozceyhan, Conjugate heat transfer and thermal stress analysis of wire coil inserted tubes that are heated externally with uniform heat flux, Energy Conversion and Management 46 (2005) 1543–1559.
R.L. Webb, R. Narayanmurthy, P. Thors, Heat transfer and friction factor characteristics of internal helical-rib roughness, Trans. ASME J. Heat Transfer 122 (2000) 134–142.
S.U.S. Choi, Enhancing thermal conductivity of fluid with nanoparticles, in: D.A. Siginer, H.P. Wang (Eds.), Developments and Applications of Non-Newtonian Flows, FED-V.231/MD-V.66, vol. 66, ASME, New York, 1995, pp. 99–105.
Yun, J. Hwang, J.T. Chung, Y. Kim, Flow boiling heat transfer characteristics of nitrogen in plain and wire coil inserted tubes, Int. J. Heat Mass Transfer 50 (2007) 2339–2345.